

X-ray Diffraction Topography on Ferroelectric Materials

Yasuhiro Yoneda, Yoshiki Kohmura¹, Yoshio Suzuki²,

Shin-ichi Hamazaki³, Masaaki Takashige⁴ and Jun'ichiro Mizuki

Synchrotron Radiation Research Center, JAERI/SPring-8, Sayo-gun, Hyogo 679-5148, Japan

Fax: 81-791-58-2740, e-mail: yoneda@spring8.or.jp

¹Harima Institute, RIKEN/SPring-8, Sayo-gun, Hyogo 679-5148, Japan

²Synchrotron Radiation Research Laboratory, JASRI/SPring-8, Sayo-gun, Hyogo 679-5198, Japan

³Fukushima National College of Technology, Iwaki, Fukushima 970-8034, Japan

⁴Department of Electronics, Iwaki-Meisei University, Iino, Fukushima 970-8551, Japan

Synchrotron radiation topography by modern radiation sources, coupled with adequate charge-coupled device (CCD) detectors, is producing in a shorter time and with better resolution results which up to now, could only be obtained, by using neutron topography. This is shown by observations, carried out at the SPring-8 using high-energy and high-flux synchrotron X-rays, of typical ferroelectric domains of BaTiO₃ crystal. The high-flux X-ray beams allowed the time-resolved experiments around the ferroelectric phase transition, and the high-energy X-rays allowed domain observation of a ferroelectric capacitor with metal electrodes.

Key words: X-ray diffraction, topography, ferroelectrics, phase transition, domain observation, BaTiO₃

1. INTRODUCTION

X-ray diffraction imaging, historically called X-ray topography, is a 'classical' technique used for the visualization of defects (dislocations, twins, domain walls, inclusions, impurity distribution *etc.*) and macroscopic deformations (curvature, acoustic waves *etc.*) present within the single-crystal sample. The first white-beam topographs, using radiation from a second-generation synchrotron sources, date back to 1974 and were made by Tuomi *et al.* [1]. Since then, numerous dedicated synchrotron radiation sources have been constructed, providing beams with higher quality and stability. The modern third-generation radiation sources offer enhanced possibilities thanks to the high energy and the low emittance of the electron beam, compared to that of previous synchrotron diffraction imaging [2,3]. Thus, diffraction topographic investigations of heavy and bulky samples and real-time experiments on a 0.05 s time scale are feasible. The low emittance implies that the source size is relatively small. These advantages can also be exploited for experiments with ferroelectric materials, especially domain observation [4-6].

Domains within a ferroelectric sample occur because they are induced by internal stress and/or as a result of the kinetics of the phase transition [7,8]. Time-resolved domain observation is a helpful investigation to understand the domain creation around the ferroelectric phase transition. Additionally, X-ray topography with hard X-rays can reveal the domain formation of a ferroelectric capacitor with metal electrodes, and high-resolution synchrotron X-ray topography can reveal the selected domain-domain correlation.

This paper shows how diffraction topography has been applied to ferroelectric materials by radiation of recent synchrotrons.

2. EXPERIMENT

As the experimental sample, a multi-domain BaTiO₃ single crystal oriented along [001], a so-called butterfly crystal prepared by Remeika's method (KF flux method) [9] was used. The crystal was polished to a final thickness of around 500 μm . Some scars and protuberances having roughness in 20 nm range were seen on the surface, which might have been formed during the growth or polishing process. However, the penetration depth of X-rays (60 ~ 70 μm) is much deeper than the surface roughness of this crystal, and so the roughness of the surface was not a serious obstacle for these X-ray measurements. After the sample was polished, gold electrodes were deposited to apply external electric field.

The X-ray topography measurements were performed at BL47XU, an undulator beamline of SPring-8. The undulator gap was 40 mm and 18 keV X-rays were used. The measurement set up is illustrated in Fig. 1. The sample crystal and its domain structure were also monitored by a visible polarization microscope. The symmetric 100 and 001 reflections were used to increase the area visible by the diffraction topography, and the Bragg angle (2θ) of the reflections was around 10 degrees at 18 keV. The reflected beam image was recorded by a 2D X-ray detector (Beam Monitor, BM) with the pixel size of 3.3 μm and the fastest shutter speed of 53 msec. The BM consisted of a fluorescent screen and a CCD (C4742, Hamamatsu Photonics Corp.). The resolution of this experimental setup with the BaTiO₃ sample was evaluated to be 20 arcsec based on the rocking curve width of the BaTiO₃ 100 reflection in the high-temperature cubic phase. It means that this experimental setup can detect an orientational difference in diffraction plane of 0.005 degree arising from the intrinsic mosaicity of the BaTiO₃ crystal.

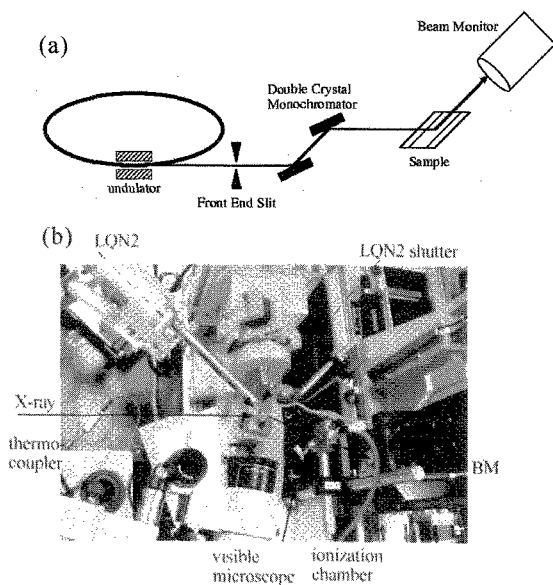


Fig. 1. (a) A schematic diagram of diffraction topography at BL47XU. (b) Experimental setup around the sample.

3. RESULTS AND DISCUSSION

3.1 Time-resolved observation around tetragonal-orthorhombic phase transition

It is well-known that BaTiO_3 undergoes a first-order phase transition at 5°C from tetragonal ($P4mm$) to orthorhombic ($C2mm$) structure. Both structures are ferroelectric states and the polar directions of tetragonal and orthorhombic phases are $[001]$ and $[110]$, respectively [10,11].

The rocking curves of the tetragonal phase at just after the phase transition and a few seconds thereafter were measured, as shown in Fig. 2. Corresponding X-ray diffraction images of the BaTiO_3 crystal are shown in Fig. 3. Figure 3(a) shows a topographic image which was taken at the peak top of the 001 tetragonal peak just after the orthorhombic-tetragonal phase transition. The images are negative, *i.e.*, white regions diffract strongly and vice versa. We continued to observe the domain configuration for a few seconds after the orthorhombic-

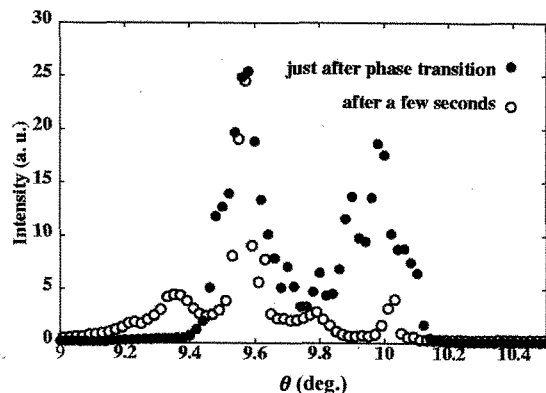


Fig. 2. Rocking curve profiles of BaTiO_3 001 reflection just after the phase transition (blackened circles) and a few seconds thereafter (open circles).

tetragonal phase transition. The sample was kept at 8°C and the 2D detector and sample positions were the same as when the topographic images of Fig. 3(a) was obtained. Figure 3(b) shows the X-ray topographic images observed 5 s after the phase transition occurred. The domain configuration of tetragonal phase was not stabilized, but rather changed drastically in a few seconds.

When the phase transition occurred, a large portion of the tetragonal c -domains was diffracted, as shown in Fig. 3(a). In the early stage of domain nucleation, small domains (seeds of the tetragonal domains) appeared. Differing lattice parameters of the tetragonal phase caused internal stress, because lattice portions different parameters were set side by side in such a small domain configuration. As a result, the rocking curve width of the early stage of domain nucleation showed broad peaks (the blackened circles of Fig. 2), and lattice strain was distributed uniformly through the whole crystal.

The lattice strain was driven to the domain boundary as the domain nucleation proceeded. The lattice strain of individual domains lessened and the rocking curve width were sharpened as shown in the open circles of Fig. 2. We have already performed preliminary experiments with the tetragonal BaTiO_3 crystal and established the relationship between the local strain at domain boundaries and coherence between domains [12,13]. In the case of the tetragonal BaTiO_3 , the lattice strain is localized at the domain boundary, and it causes fluctuation in the mode of the surface bending and tilting of the polar direction. Thus, the domain-domain correlation was broken and only a part of the c -domains caused diffraction at the final stage of the domain nucleation, as in Fig. 3(b).

In ferroelectrics, the phase transition is affected by constraints, for example, strain at domain boundaries and strain due to defects, impurities and dislocations. The presence or absence of the pinning state at a low temperature phase may be different in individual domains, and the transition temperature also may well be different in different individual domains. Thus, the domain size of the high-temperature phase was greatly suppressed in the early stage of domain nucleation.

With regard to individual domains, the lattice strain moved to domain boundaries and it was reduced inside the domain as the domain size became larger. On the other hand, the lattice strain was concentrated at the domain boundary, with affected the domain-domain correlation as the domain nucleation proceeded. The polar direction of a domain is tilted from those of the

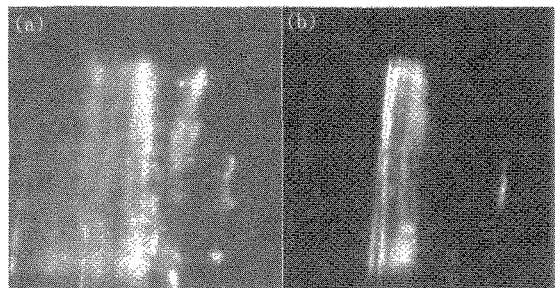


Fig. 3. X-ray diffraction topography images of BaTiO_3 crystal with c -domains. (a) and (b) are images observed just after the phase transition and a few seconds thereafter, respectively.

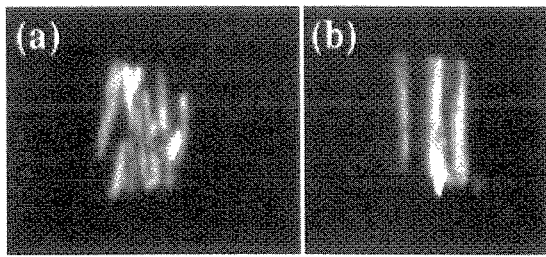


Fig. 4. X-ray diffraction topography of BaTiO_3 crystal. (a) shows the topographic image of orthorhombic phase observed at $T = 0^\circ\text{C}$. (b) shows the topographic image of electric-field induced transition tetragonal phase at $T = 0^\circ\text{C}$.

other domains due to the lattice strain at the domain boundary. In the case of small domains, the crystal quality is affected by the lattice strain inside the domain. In the large domains, the polar direction is affected by the lattice strain from the domain boundary. It is necessary to control both lattice strain and crystal quality to obtain novel ferroelectric materials, using domain-engineering techniques.

3.2 Electric-field induced tetragonal-orthorhombic phase transition

Next, we tried to pole a sample in a low-temperature orthorhombic phase. The electrodes were attached on the [001] surface which can change the polar direction of the tetragonal phase, but which cannot switch the orthorhombic domain. Figure 4(a) shows the topographic image observed at $T = 0^\circ\text{C}$ and $E = 0\text{ V}$. The external field was increased and when the field voltage was 5.0 kV/cm , the domain configuration was completely changed, as shown in Fig. 4 (b). The external electric field changed the BaTiO_3 crystal from the orthorhombic to the tetragonal phase. The domain configuration of Fig. 4(b) is similar to the stripe pattern of the tetragonal phase, and the diffracted areas of Fig. 4(b) were c -domains (*i.e.*, whose polar c -axis is normal to the crystal surface in the tetragonal phase).

Observation of the domain under the gold electrodes were successfully carried out. Even if the BaTiO_3 was transformed by the electric field, the domain configuration of the tetragonal phase was not a single domain, but the usual stripe pattern. The interval between the stripes in the formed domains was very close to that of the tetragonal phase which observed at room temperature. When the tetragonal-orthorhombic phase transition occurred, the orthorhombic domain was generated within the tetragonal domain as illustrated in Fig. 5. Thus, a trace of the tetragonal domain configuration was retained even in the low-temperature orthorhombic phase.

Before this experiment, we considered that the domain configuration that is transformed by the electric field would be a single domain, because we thought the applied electric field would be sufficient to align the polar directions. However, the transformed domain pattern comprised cancelled stripe domains. It is necessary to apply larger electric field to make a complete single domain. The electrodes had been put on the [001] surface of the BaTiO_3 crystal, because for the [110] polarization into the orthorhombic phase, it was

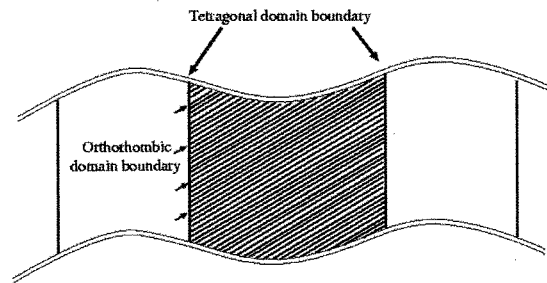


Fig. 5. A schematic diagram of domain nucleation around the phase transition.

difficult to rotate the [001] direction, than to transform to the tetragonal phase.

In the experiments of the previous subsection, the BaTiO_3 sample passed the orthorhombic-tetragonal phase transition many times. Each time, the domain pattern of the tetragonal phase was reproduced precisely. This is surprising, because in addition to the fact that the domain patterns of ferroelectric crystals are affected by defects and/or impurities, a trace of the domain pattern of the higher-temperature phase is retained in the lower-temperature phase. It should be very difficult to change the domain pattern of ferroelectric crystals simply by changing temperature.

In the case of domain nucleation under an electric field, the pattern of the domains transferred to the tetragonal phase reproduced the stripe pattern of the normal tetragonal phase. Although the domain pattern was not changed, the magnitude of the lattice strain in individual domains was different from that in the normal tetragonal phase. The transformed BaTiO_3 crystal was free from the lattice strain caused by small domains (seeds of domains), and so the crystal quality of the individual domains were improved. This indicates that the lattice strain in the c -domains was driven to the a -domains. The crystal quality of the c -domains was improved at the expense of the a -domains. Therefore, the coherence between domains was significantly injured in the transformed tetragonal domains. This fact explains the difference in the rocking curve profiles of these tetragonal domains.

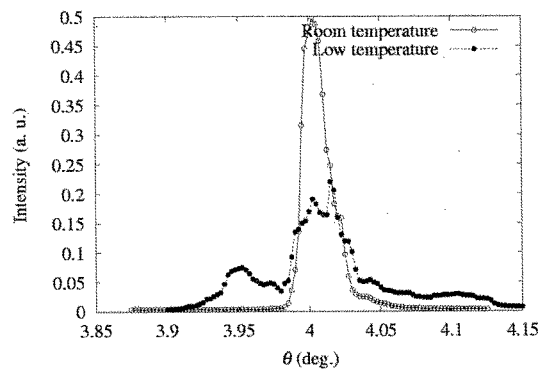


Fig. 6. Rocking curve profiles of BaTiO_3 001 reflection of normal tetragonal phase (open circles) and tetragonal phase transformed by an external electric field (blackened circles).

Figure 6 shows the rocking curve profiles of *c*-domains in the normal tetragonal phase and in the transformed tetragonal phase. The rocking curve width of the transformed tetragonal domain was broader than that of the normal tetragonal domain. The reflection of the force-transferred tetragonal domain split in two peaks and was diffuse, indicated that the large strain from the *a*-domains broke the coherence between the *c*-domains. This type of strain is likely the origin of the difficulty of forming a single domain. The *a*-domain of the transformed tetragonal phase is necessary for the escape of the lattice strain inside the domains.

Recently, there has been increased interest in the possibility that some types of domains have lower transition temperature and higher dielectric response than the field-free monodomain state [14]. Many attempts at domain engineering (e.g. field cooling) have been made to obtain novel ferroelectric materials. Our experimental results may provide a good suggestions for domain engineering with field cooling/heating. Field cooling holds much promise for obtaining different domain configuration. Because the domain pattern of a high-temperature phase may be changed to a monodomain by an electric field, it should be possible to effect the domain evolution of the low-temperature phase free from any traces of high-temperature domain configuration.

4. CONCLUSIONS

X-ray diffraction imaging is today a 'classical' technique. It is, of course, still very useful in its original form for characterizing single crystals of ferroelectric materials. However, in addition, the association with modern synchrotron radiation sources has expanded its usefulness. It is presently partly used to follow *in-situ* and/or real-time phenomena, *i.e.* the evolution of a process as a function of an external parameter (time, temperature, electric field *etc.*).

Our experimental results provide informations of use in solving important problems of domain engineering: (1) traces of the domain configuration of the high-temperature phase remain in the low-temperature phase, (2) it is necessary to anneal the ferroelectric material at a higher-temperature phase to change or reset the low-temperature domain configuration, and (3) in the case that the domain nucleation is prevented by defects and/or impurities, the domain configuration is difficult to change even if it is annealed at a higher-temperature phase.

ACKNOWLEDGMENT

The synchrotron radiation experiments were performed at the BL47XU in the SPring-8 with the approval of the Japan Synchrotron Radiation Research Institute (JASRI)(Proposal No. 2002A0059-NM-np).

REFERENCES

- [1] T. Tuomi, K. Naukkarinen, and P. Rabe, *Phys. Status Solidi A*, **25**, 93-106 (1974).
- [2] J. Baruchel, P. C. de Camargo, H. Klein, I. Mazzaro, J. Nogues, and A de Oliveira, *J. Phys. D: Appl. Phys.* **34**, A114-A116 (2001).
- [3] J. Baruchel, J. Hartwig, and P. Pernot-Rejmankova, *J. Synchrotron Rad.* **9**, 107-114 (2002).
- [4] Z. H. Hu, P. A. Thomas, A. Snigirev, I. Snigireva, A. Souvorov, P. G. R. Smith, G. W. Ross, and S. Teat, *Nature* **392**, 690-693 (1998).
- [5] M. Drakopoulos, Z. W. Hu, S. Kuznetsov, A. Snigirev, I. Snigireva, and P. A. Thomas, *J. Phys. D: Appl. Phys.* **32**, A160-A165 (1999).
- [6] J. Baruchel, P. Cloetens, J. Hartwig, W. Ludwig, L. Mancini, P. Pernot, and M. Sclenker, *J. Synchrotron Rad.* **7**, 196-201 (2000).
- [7] S. Hamazaki, F. Shimizu, S. Kojima, and M. Takashige, *J. Phys. Soc. Jpn.* **64**, 3660-3663 (1995).
- [8] M. Takashige, S. Hamazaki, Y. Takahashi, F. Shimizu, and T. Yamaguchi, *Jpn. J. Appl. Phys.* **38**, 5686-5688 (1999).
- [9] J. P. Remeika, *J. Amer. Chem. Soc.* **76**, 940-941 (1954).
- [10] P. W. Forsbergh, Jr., *Phys. Rev.* **76**, 1187-1201 (1949).
- [11] F. Jona, and G. Shirane, *International Series of Monographs on Solid State Physics Vol. 1, Ferroelectric Crystals* (Pergamon Press, Oxford, London, New York, Paris, 1962) p. 162.
- [12] Y. Yoneda, Y. Kohmura, Y. Suzuki, S. Hamazaki, and M. Takashige, *J. Phys. Soc. Jpn.* **73**, 1050-1053 (2004).
- [13] Y. Yoneda, J. Mizuki, Y. Kohmura, Y. Suzuki, S. Hamazaki, and M. Takashige, *Jpn. J. Appl. Phys.* **43**, 6821-6824 (2004).
- [14] Y. Watanabe, M. Okano, and A. Masuda, *Phys. Rev. Lett.* **86**, 332-335 (2001).

(Received December 23, 2004; Accepted January 31, 2005)